

Transition from Homogeneous Langmuir–Blodgett Monolayers to Striped Bilayers Driven by a Wetting Instability in Octadecylsiloxane Monolayers

Michael C. Howland,[†] Malkiat S. Johal,^{*,‡} and Atul N. Parikh^{*,†}

Department of Applied Science, University of California, Davis, California 95616, and
Division of Natural Sciences, New College of Florida, Sarasota, Florida 34243

Received March 20, 2005. In Final Form: August 6, 2005

We show that two dips of an oxidized silicon substrate through a prepolymerized *n*-octadecylsiloxane monolayer at an air–water interface in a rapid succession produces periodic, linear striped patterns in film morphology extending over macroscopic area of the substrate surface. Langmuir monolayers of *n*-octadecyltrimethoxysilane were prepared at the surface of an acidic subphase (pH 2) maintained at room temperature (22 ± 2 °C) under relative humidities of 50–70%. The substrate was first withdrawn at a high dipping rate from the quiescent aqueous subphase (upstroke) maintained at several surface pressures corresponding to a condensed monolayer state and lowered soon after at the same rate into the monolayer covered subphase (downstroke). The film structure and morphology were characterized using a combination of optical microscopy, imaging ellipsometry, and Fourier transform infrared spectroscopy. An extended striped pattern, perpendicular to the pushing direction of the second stroke, resulted for all surface pressures when the dipping rate exceeded a threshold value of 40 mm min⁻¹. Below this threshold value, uniform deposition characterizing formation of a bimolecular film was obtained. Under conditions that favored striped deposition during the downstroke through the monolayer-covered interface, we observed a periodic auto-oscillatory behavior of the meniscus. The stripes appear to be formed by a highly correlated reorganization and/or exchange of the first monolayer, mediated by the Langmuir monolayer at the air–water interface. This mechanism appears distinctly different from nanometer scale stripes observed recently in single transfers of phospholipid monolayers maintained near a phase boundary. The stripes further exhibit wettability patterns useful for spatially selective functionalization, as demonstrated by directed adsorptions of an organic dye (fluorescein) and an oil (hexadecane).

Introduction

Langmuir–Blodgett (LB) films built by the controlled transfer of equilibrium monolayers of insoluble amphiphiles from the air–water interface¹ to a solid surface have been studied for almost a whole century.^{2,3} Despite considerable experimental and theoretical effort, fabricating uniform, defect-free films with predictable structural properties continues to pose a significant challenge.^{4,5} This is so because defects form due to instabilities associated with the transfer process and/or monolayer reorganizations at the substrate surface due to shifts in equilibrium properties. A full spectrum of defect structures including isolated pinholes, domain boundaries, topographical inhomogeneities, missing domains, and layering irregularities have been reported within LB assemblies. Under certain experimental conditions, these instabilities can give rise to interesting features (e.g., uniform stripes and striations) that can be exploited for patterning substrate wettabilities and thus functionalities.^{6–16}

Correlated reorganizations of transferred Langmuir monolayers have yielded interesting classes of bubble and striped morphologies. In a recent study, Moraille and Badia⁹ have shown that selected compositions, a fluid-phase phospholipid, DLPC (1,2-dilauroyl-*sn*-glycero-3-phosphocholine), and a solid-phase lipid, DPPC (1,2-dipalmitoyl-*sn*-glycero-3-phosphocholine), can reorganize via directed phase separation processes during the LB transfers to form solid/liquid alternating striped patterns of DPPC and DLPC, respectively. Alternatively, meniscus oscillations induced by competing influences of hydrodynamic and intermolecular forces have been shown to result in controllable striped morphologies of the single LB monolayers. For example, Gleiche et al.⁷ have suggested that substrate-induced phase condensation in conjunction with hydrodynamic instabilities results in nanoscale stripe formation. Specifically, they observe that a single monolayer transfer from the liquid-expanded (LE) Langmuir phase of DPPC at low surface pressures (~ 3 mN m⁻¹) onto a mica substrate at rapid transfer velocities (~ 60

* Corresponding author. Phone: (530) 754-7055. Fax: (530) 752-2444. E-mail: anparikh@ucdavis.edu.

[†] University of California.

[‡] New College of Florida.

(1) Gaines, G., Jr. *Insoluble Monolayers at Liquid–Gas Interfaces*; John Wiley & Sons: New York, 1966.

(2) Ulman, A. *An Introduction to Ultrathin Organic Films: From Langmuir–Blodgett to Self-Assembly*; Academic Press: San Diego, CA, 1991.

(3) Schwartz, D. K. *Surf. Sci. Rep.* **1997**, *27*, 245–334.

(4) Peterson, I. R. *J. Phys. D: Appl. Phys.* **1990**, *23*, 379–395.

(5) Zasadzinski, J. A.; Viswanathan, R.; Madsen, L.; Garnæs, J.; Schwartz, D. K. *Science* **1994**, *263*, 1726–1733.

(6) Spratte, K.; Chi, L. F.; Riegler, H. *Europhys. Lett.* **1994**, *25*, 211–217.

(7) Gleiche, M.; Chi, L. F.; Fuchs, H. *Nature* **2000**, *403*, 173–175.

(8) Mahnke, J.; Vollhardt, D.; Stockelhuber, K. W.; Meine, K.; Schulze, H. *J. Langmuir* **1999**, *15*, 8220–8224.

(9) Moraille, P.; Badia, A. *Langmuir* **2002**, *18*, 4414–4419.

(10) Moraille, P.; Badia, A. *Langmuir* **2003**, *19*, 8041–8049.

(11) Kovalchuk, V. I.; Zholkovskiy, E. K.; Bondarenko, M. P.; Vollhardt, D. *J. Phys. Chem. B* **2004**, *108*, 13449–13455.

(12) Kovalchuk, V. I.; Kamusewitz, H.; Vollhardt, D.; Kovalchuk, N. M. *Phys. Rev. E* **1999**, *60*, 2029–2036.

(13) Merle, H. J.; Alberti, B.; Schwendler, M.; Peterson, I. R. *J. Phys. D: Appl. Phys.* **1992**, *25*, 1556–1558.

(14) Eriksson, L. G. T.; Claesson, P. M.; Ohnishi, S.; Hato, M. *Thin Solid Films* **1997**, *300*, 240–255.

(15) Purrucker, O.; Fortig, A.; Ludtke, K.; Jordan, R.; Tanaka, M. *J. Am. Chem. Soc.* **2005**, *127*, 1258–1264.

(16) Moraille, P.; Badia, A. *Angew. Chem., Int. Ed.* **2002**, *41*, 4303–4306.

mm min⁻¹) gives rise to stripes comprising 0.8 μm monolayer domains separated by 0.2 μm channels. Mahnke et al.,⁸ on the other hand, have suggested that concentration polarization within the solution during the transfer of charged amphiphiles¹¹ can couple with the hydrodynamic instabilities to produce micrometer scale striped morphologies. They demonstrated these electrohydrodynamic instability driven stripe formation using arachidic acid monolayer (surface pressure 30 mN m⁻¹) transfers at slow speeds (3–8 mm/min) in the presence of cadmium chloride.

In this work, we show that two successive passes of an oxidized silicon (SiO₂/Si) substrate through a precompressed, prepolymerized Langmuir monolayer of *n*-octadecyl trimethoxysilane (OTMS) produce periodic, linear striped patterns in film morphology, parallel to the three phase interface. The stripes appear to be formed by a highly correlated reorganization of the first monolayer in conjunction with hydrodynamic meniscus oscillation during the downstroke of the monolayer covered substrate. Furthermore, these stripes exhibit topographic and wettability contrasts, which we exploit for spatially selective functionalizations.

Experimental Section

Materials. The materials *n*-octadecyltrimethoxysilane (OTMS; 90% purity, Acros Organic, Morris Plains, NJ), ACS grade chloroform, ethanol, and methanol (>99% purity) were purchased from Aldrich (Milwaukee, WI) and used as received. Sodium fluorescein acquired from Sigma (St. Louis, MO) and iron(III) nitrate from Alfa Aesar (Ward Hill, MA) were also used as received. Nitric acid used as a Langmuir subphase was purchased from EM Science (Gibbstown, NJ) and diluted to 10⁻² M. For all cleaning, dilutions, and deposition procedures, deionized (DI) water (resistivity > 18.0 M Ω cm) was used. Organic-free deionized water was obtained by processing water through a Millipore purification system (Bedford, MA) consisting of a reverse osmosis deionization cartridge and an ion exchange/carbon purification system. All glassware used was thoroughly precleaned using Alconox detergent (Alconox, New York, NY) followed by extensive washing with deionized water, low organic-content water, and finally air-dried in a glassware oven maintained at ~110 °C. Test-grade silicon wafers (0.28 mm thick) that were polished on a single side (Silicon Sense, Inc., Nashua, NH) were typically used as substrates. The 2" round wafers were cut to 35 mm on three sides, leaving the rounded side for attachment to the substrate holder used for LB dips. For the Fourier transform infrared (FT-IR) spectroscopy measurements, 1 mm thick square plates consisting of low-dopant silicon with ~20 Å native oxide overlayer (SiO₂/Si) obtained from Harrick Scientific (Ossining, NY) were used. Both sides were finished to a high polish, and one side was wedged slightly off-parallel from the other by 0.25° to minimize the interference fringes in the transmission infrared spectroscopy measurements.

Substrate Pretreatment. All SiO₂/Si substrates were thoroughly degreased by ultrasonication in ethanol for ~2 min. The samples were then oxidized¹⁷ using either chemical (piranha-etch treatment) or photochemical (UV/ozone oxidation). Both cleaning processes yielded identical results. The piranha-etch treatment involved immersing the samples for a period of 5–10 min in a freshly prepared 4:1 v/v mixture of sulfuric acid (A300–500, Fisher Certified ACS+, Fairlawn, NJ) and hydrogen peroxide (30%, EM Science, Gibbstown, NJ) maintained at ~90–110 °C. (*Caution: This mixture reacts violently with organic materials and must be handled with extreme care.*) The samples were then withdrawn using Teflon tweezers and rinsed immediately with a copious amount of DI water. Substrates were stored under DI water until used. Alternatively, UV/ozone treatment¹⁸ was carried out by placing SiO₂/Si substrates 6–10 mm from the UV lamp in a UVOCS model T06063 UV/Ozone cleaning system (Mont-

gomeryville, PA) or a home-built UV/Ozone reactor housing an ozone-generating medium-pressure Hg lamp in a quartz envelope (UVP Inc., Upland, CA) maintained under ambient conditions. The samples were exposed to the ozone generating short-wavelength UV radiation (187–254 nm) for 15 min. The UV/ozone treated samples were then rinsed thoroughly using DI water and dried under nitrogen prior to LB deposition.

Isotherm Measurements and Langmuir–Blodgett Transfers. All Langmuir film preparations, isotherm measurements, and LB depositions were carried out using a computer controlled Langmuir trough (model 611, NIMA Technologies, Coventry, England) made of poly(tetrafluoroethylene) (PTFE). The moving barriers were Teflon-coated, and the surface pressure (Π) measurements were made by the Wilhelmy plate method using a 21 mm perimeter plate cut from a filter paper.

A previously described procedure was followed for LB deposition.¹⁹ The subphase consisted of 0.2 M nitric acid with a pH of ~2. The temperature of the ambient medium (air) was not controlled. Ambient relative humidity ranged from 50.9% to 69.0%. 30 μL aliquots of the monomeric, OTMS solutions (2.6 mg/mL in 5% methanol/95% chloroform) were applied to the freshly aspirated surface of the subphase. A low pH acidic subphase was used to foster surface gelation of OTMS molecules at the aqueous interface. The acidic conditions near the isoelectric point for the film are known to allow rapid and complete hydrolysis of the trimethoxy headgroup to –Si(OH)₃ but relatively slow formation of Si–O–Si cross-links.²⁰ The subphase surfaces were left standing for at least 25 min to allow complete solvent evaporation and subsequent hydrolysis and polymerization of the trimethoxy headgroup at ~0 mN m⁻¹ barrier pressure. Considerably longer standing times do not change the isotherm characteristics in any noticeable way, suggesting complete polymerization. The subphase temperature during the isotherm was not controlled, but was typically 22 ± 2 °C.

LB depositions occurred isothermally in the upstroke/downstroke sequence at desired surface pressure values and dipping velocities. The prepolymerized OTMS Langmuir monolayers were slowly compressed to desired surface pressures by reducing the trough perimeter using motor-driven barrier compression at the rate of 40 cm² min⁻¹. At the desired surface pressure values, the Langmuir monolayers were allowed to equilibrate for ~15 min. Pre-immersed SiO₂/Si substrates were first drawn up through the air–subphase interface (upstroke), and then pushed back down through the interface and into the subphase (downstroke). The delay between the upstroke and the downstroke was typically 5 min. The air–subphase interface was aspirated after the downstroke, resulting in zero surface pressure. The barriers were relaxed before finally withdrawing the sample from the subphase. The strokes occurred at surface pressures of 10, 20, 35, and 40 mN m⁻² and at dipping rates of 5, 20, 50, and 60 mm min⁻¹. The samples were air-dried before characterization unless noted otherwise.

Imaging Ellipsometry. Ellipsometric contrast images were acquired using a commercial, null imaging ellipsometer (iElli 2000, Nanofilm Technologie). The ellipsometer was operated at 532 nm using a frequency-doubled Nd:YAG laser (adjustable power up to 20 mW) and equipped with a motorized goniometer for an accurate selection of the incidence angle. The ellipsometer employed a PCSA nulling-configuration in which a linear polarizer (P) and a quarter-wave plate (C) yield an elliptically polarized incident beam. Upon reflection from the sample (S), the beam was gathered via an analyzer (A) and imaged onto a CCD camera through a long working distance 10× or 20× objective. The P, C, and A positions that yielded the null condition were then converted to the ellipsometric angles, Δ and Ψ . An incidence angle of 60° was used for all measurements.

Ellipsometric angles were transformed into film optical thicknesses using the iElli2000 software based on the standard electromagnetic treatment for a parallel-layer model.²¹ The samples were approximated to consist of a four layered, air/

(19) Wood, J.; Sharma, R. *Langmuir* **1994**, *10*, 2307–2310.

(20) Devreux, F.; Boilot, J. P.; Chaput, F.; Lecomte, A. *Phys. Rev. A* **1990**, *41*, 6901–6909.

(21) See, for example: Azzam, R. M. A.; Bashara, N. M. *Ellipsometry and Polarized Light*; North-Holland: Amsterdam, The Netherlands, 1977.

(17) Frantz, P.; Granick, S. *Langmuir* **1992**, *8*, 1176–1182.

(18) Vig, J. R. *J. Vac. Sci. Technol., A* **1985**, *3*, 1027–1034.

OTMS film/SiO₂/Si structure. In the present implementation of null-ellipsometry (single wavelength and single incidence angle measurements), the application of the optical model requires independent assignments of the thickness of the SiO₂ phase and refractive indices for all layers. The thickness of the SiO₂ was assumed to be 20 Å, consistent with the values determined in three-phase models for the ellipsometric measurements of film-free substrates. Refractive indices of Si and SiO₂ at 532 nm were 4.1502 - 0.0449i and 1.4608 + 0.0i, respectively. The refractive index for the OTMS layer was assumed to be 1.45 + 0.0i on the basis of previous studies.²²

Spatially resolved measurements of ellipsometric angles yielded 3D maps of the ellipsometric angle, Δ . In a typical mapping experiment, 10–20 images were taken over a 4° rotation of the polarizer. These images were then assembled to find the null (lowest intensity) for each point.²³ Spatially resolved Δ values were then computed from these null conditions. Spatial resolution in the images is determined by the collection objective placed before the CCD camera. 10× objectives yielded 2 μm lateral resolution and 641 × 430 μm image dimensions. For 3D maps, pixels were binned in 2 × 2 squares, resulting in the final lateral resolution of 4 μm. Finally, thickness values were derived using the parallel slab model described above. 3D images and contour maps revealing surface profiles of ellipsometric thicknesses were then generated using SigmaPlot software (SPSS Inc., Chicago, IL).

FT-IR Spectroscopy. Transmission infrared spectra were obtained using a FT-IR spectrometer (Bruker Optics, Equinox IFS 55, Tubingen, Germany) operating at 4 cm⁻¹ resolution with an unpolarized, convergent beam transmitting through the sample surface at normal incidence angle. The beam diameter at the focus was fixed at 10 mm by an aperture. The resulting interferograms from 400 co-added scans were Fourier transformed with Blackman–Harris-three term apodization technique and zero-filling to increase the point density by a factor of 4, which yields an effective resolution of ~1 cm⁻¹ for an accurate determination of the peak positions. The spectra of LB films were referenced against the spectra obtained for the same clean, bare substrate wafers before the Langmuir deposition. All spectra are reported in absorbance units, $-\log(T/T_0)$, where T and T_0 are the emission power spectra of each sample and reference, respectively.

Stripe Functionalization. LB bilayers displaying stripe morphologies were further characterized using three functionalization processes involving simple chemical depositions and photochemical treatments. The photochemical treatment involved simply the exposure of LB striped samples to ozone generating short-wavelength UV radiation using a grid-Hg lamp in quartz envelope (see above). Samples were placed in close proximity (below 10 mm) to the UV source and irradiated for approximately 90 min. The photochemical treatment is expected to degrade the film alkyl chain leaving behind the silicon oxide.²⁴ The patterns of silicon oxide can then be used to characterize the striped pattern in terms of monolayer coverage. Chemical film functionalizations were carried out by spin-coating the striped LB bilayer samples with sodium salt of fluorescein isothiocyanate (FITC), iron (III) nitrate, and hexadecane. Ethanolic solutions of FITC and iron salts in arbitrary concentrations (well below saturation values) and pure hexadecane were placed on the LB bilayer samples spinning at 3000 rpm. Briefly, the samples were first accelerated to 3000 rpm using Chemat KW-4A spin-coater (Chemat Technology, Inc., Northridge, CA). Subsequently, small aliquots (~1 mL) of solutions were dropped onto the spinning sample. The samples were spun for an additional 25 s. After spin-coating, the samples were characterized using optical microscopy and imaging ellipsometry to examine for any pattern amplification resulting from the deposition preferences.

Results

OTMS Monolayers at the Air–Water Interface. It is now well-established that long-chain trialkoxysilanes

(22) Parikh, A. N.; Allara, D. L.; Azouz, I. B.; Rondelez, F. *J. Phys. Chem.* **1994**, *98*, 7577–7590.

(23) A point consisted of a 2 × 2 group of pixels binned together.

(24) Dulcey, C. S.; Georger, J. H.; Krauthamer, V.; Stenger, D. A.; Fare, T. L.; Calvert, J. M. *Science* **1991**, *252*, 551–554.

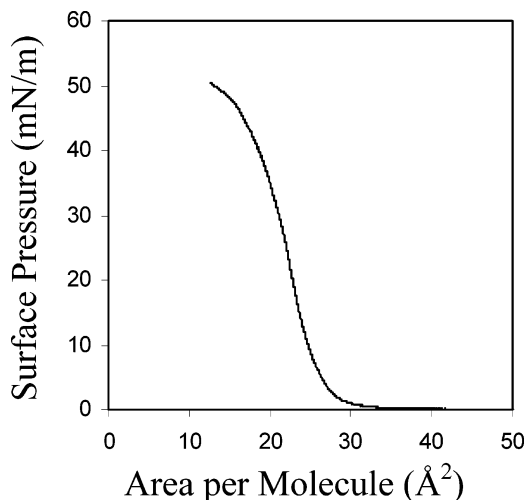


Figure 1. Surface pressure (mN m^{-1})–molecular area ($\text{Å}^2/\text{molecule}$) isotherm of *n*-octadecyltrimethoxysilane on a nitric acid subphase at pH 2 under room-temperature conditions.

undergo a strong pH-dependent two-dimensional (2D) surface polymerization at the air–water interface.^{25–28} The polymerization involves a complex sequence of headgroup hydrolysis and intermolecular condensation reactions, both of which depend strongly on subphase pH as well as monolayer density (or surface pressure) and incubation time. At very low (<1.5) and high (>11) pH values, a polymerized viscoelastic phase readily emerges via rapid hydrolysis–condensation reactions.²⁹ By contrast, in the vicinity of the isoelectric point of the film, ~3.0–3.8, the condensation reaction is considerably slowed. Under these conditions, the hydrolysis of trimethoxy headgroup continues to be rapid ensuring high surface populations of trihydroxysilyl precursors.³⁰ On the basis of the above, we reasoned that the subphase pH of 2 should provide effective separation of hydrolysis and condensation reactions, thereby allowing slow condensation to produce uniform Langmuir films. Long time scales of our experiment (>60 min including solvent evaporation and surface equilibration times) in conjunction with compression-induced increase in molecular density ensure high intermolecular condensation prior to film deposition.

A typical Π – A isotherm for the Langmuir films derived from OTMS monolayers on an aqueous subphase of pH ~2 at room temperature is shown in Figure 1. The isotherm is characterized by three distinct regions. The initial flat portion of the isotherm extends from 80 to 27 $\text{Å}^2/\text{molecule}^{-1}$ at approximately $\Pi = 0$. This region is comparable to the 2D gas phase for classical amphiphiles.³¹ Because a significant prepolymerization is expected to have occurred prior to compression,³² the region corresponds to a molecular picture wherein prepolymerized clusters diffuse independently. At ~34 $\text{Å}^2/\text{molecule}^{-1}$, we observe the onset of the second region of the isotherm characterized by a

(25) Linden, M.; Slotte, J. P.; Rosenholm, J. B. *Langmuir* **1996**, *12*, 4449–4454.

(26) Vidon, S.; Leblanc, R. M. *J. Phys. Chem. B* **1998**, *102*, 1279–1286.

(27) Taylor, D. M.; Gupta, S. K.; Dynarowicz, P. *Thin Solid Films* **1996**, *285*, 80–84.

(28) Sjöblom, J.; Stakkestad, G.; Ebeltoft, H.; Friberg, S. E.; Claesson, P. *Langmuir* **1995**, *11*, 2652–2660.

(29) Britt, D. W.; Hlady, V. *J. Phys. Chem. B* **1999**, *103*, 2749–2754.

(30) Okahata, Y.; Yokobori, M.; Ebara, Y.; Ebato, H.; Ariga, K. *Langmuir* **1990**, *6*, 1148–1153.

(31) Knobler, C. M. *Science* **1990**, *249*, 870–874.

(32) Ybert, C.; Lu, W. X.; Moller, G.; Knobler, C. M. *J. Phys.: Condens. Matter* **2002**, *14*, 4753–4762.

sharp increase in surface pressure as the monolayer is compressed further. This increase in pressure is consistent with the formation of liquid-condensed phase. As the area is decreased below $27 \text{ \AA}^2 \text{ molecule}^{-1}$, a change of slope characterizes the incipient third regime of the monolayer. Here, the slope decreases rapidly leading to a plateau near 50 mN m^{-1} . This behavior is consistent with the monolayer collapse typically associated with the loss of 2D character of the Langmuir monolayer by overturning of jammed molecules (and clusters) nucleating a three-dimensional mesophase.³² The isotherm characteristics noted here are in excellent agreement with those reported previously.^{26,33,34}

Several features of the isotherm presented in Figure 1 are particularly relevant for the present study. First, the isotherm reveals the notable absence of the liquid-expanded (LE) phase. Absence of the LE phase suggests that upon compression, the growth of OTMS film occurs by aggregation of LC islands as opposed to the conformational transitions that characterize isotherms of typical amphiphiles.³¹ This scenario is consistent with the expected high hydrolysis and condensation of the trimethoxy headgroup under conditions used here. Upon hydrolysis, the trimethoxy headgroup is replaced by a trihydroxy-headgroup, which is significantly smaller and essentially neutral at pH 2 (close to isoelectric point). Next, the condensation of the hydrolyzed precursors renders the aliphatic chain substituents rigid due to severe steric constraints.^{35,36} Thus, it is reasonable to suggest that aggregates formed at low surface pressures float randomly over the available surface area in a 2D phase until compressed to very small molecular areas when cluster-cluster interactions drive the formation of the condensed phase. Second, we note that the mean molecular area for the condensed OTMS phase is $25\text{--}27 \text{ \AA}^2 \text{ molecule}^{-1}$, noticeably higher than the values of $19\text{--}21 \text{ \AA}^2 \text{ molecule}^{-1}$ typically observed for silane monolayers formed at near neutral pH. This feature further supports the notion that significant surface gelation has occurred. Aggregates and clusters formed due to surface gelation render the notions of mean molecular area somewhat unphysical especially when the cluster sizes are polydisperse. Indeed, the formation of ring structures as well as star-shaped morphologies has been proposed for the early stages of OTMS polymerization under acidic conditions.³⁷ Third, we note that the absence of the LE phase makes structures of the precursor Langmuir monolayer self-consistent at all surface pressures differing only in molecular densities.

Preparation and Characterization of the Proximal OTMS Monolayer. Deposition of the first monolayer was achieved by withdrawing pre-immersed SiO_2/Si surfaces through the monolayer-covered air-water interface. SiO_2/Si substrates were cleaned immediately before the experiment began, and the surface monolayer was maintained at various surface pressures between $\Pi = 10\text{--}40 \text{ mN m}^{-2}$ ($10, 20, 35, 40 \text{ mN m}^{-2}$) and the dipping rates were varied between 5 and 60 mm min^{-1} ($5, 20, 50, 60 \text{ mm min}^{-1}$). In all cases, the Langmuir-Blodgett transfers resulted in high transfer ratios, indicating an efficient transfer of molecules from the trough surface to the substrate.

When the films were dipped at low rates ($<40 \text{ mm min}^{-1}$), the substrates emerged completely dry (autophobic). Specifically, the films exhibited high water contact angles ($>100^\circ$) and revealed the expected $25\text{--}28 \text{ \AA}$ ellipsometric thicknesses, suggesting the formation of a single OTMS monolayer. These results are in excellent agreement with those reported previously.^{19,22} When the films were dipped at higher rates ($>40 \text{ mm min}^{-1}$), however, the surfaces were visibly wet for several minutes following the withdrawal from the subphase. This may be due to the presence of entrained water at the monolayer-substrate interface. The observation is consistent with the notion that at high dipping speeds, the contact angle between the meniscus and substrate may drop below the so-called "zipper angle". The zipper angle, as described by Langmuir,³⁸ is the angle above which water is readily expelled from the film due to the attractive force between the film and substrate. Deposition of films below the zipper angle results in incomplete drainage and entrapment of water at the monolayer/substrate interface. It was also noted in that study that entrapped water may be very thick, occasionally as thick as several micrometers, and may prevent the film from bonding to the surface for several minutes before the drainage is complete.

Preparation and Characterization of the Second LB Monolayer. The distal leaflet of the LB bilayers was prepared under conditions that favored meniscus auto-oscillations. This requires dipping speeds greater than 40 mm min^{-1} and $3\text{--}5 \text{ min}$ intermission between the strokes. The latter wait-time was necessary to ensure that the substrates were visibly dry. At the same time, we observed that longer wait times ($>5 \text{ min}$) prevented meniscus oscillations, presumably due to the covalent coupling of the proximal OTMS monolayer to the SiO_2/Si substrate. Strikingly low transfer ratios were obtained for the downstroke for all samples during the deposition process. In a typical run, the transfer ratios were close to 0.003 ± 0.010 . This result suggests that little or no net deposition occurred during the downstroke.

Once removed from the freshly aspirated subphase, the dried samples were optically clear. A simple condensation or breath test, such as obtained by exposure to water vapor,³⁹ revealed a remarkably periodic stripe morphology over much of the substrate surface. Upon removal from a high vapor-pressure environment, the pattern erased quickly (within a few seconds) as the condensed water evaporated. Because hydrophilic regions of the samples favor water condensation, the patterns observed here suggest that linear stripes of alternating hydrophilicity are produced by the LB depositions described above. These stripes are aligned perpendicular to the dip direction and extend over the entire sample surface. Rotation of the sample by 90° between the first and second dipper stroke did not inhibit stripe formation. The striped domains remained perpendicular to the push direction of the second dipper stroke. This suggests the phenomenon is not an artifact of the first deposition such as the striped domains observed in numerous other systems.^{7-9,14} Stripe formation was not observed when the downstroke of the monolayer-coated substrate occurred through an OTMS free air-water interface. This control suggests the requirement of the OTMS present at the air-water interface. Additional control experiments wherein the sample was removed from the subphase at varying angles did not inhibit stripe

(33) Brousseau, J. L.; Vidon, S.; Leblanc, R. M. *J. Chem. Phys.* **1998**, *108*, 7391-7396.

(34) Blaudez, D.; Bonnier, M.; Desbat, B.; Rondelez, F. *Langmuir* **2002**, *18*, 9158-9163.

(35) Wang, R. W.; Baran, G.; Wunder, S. L. *Langmuir* **2000**, *16*, 6298-6305.

(36) Wang, R. W.; Wunder, S. L. *Langmuir* **2000**, *16*, 5008-5016.

(37) Fontaine, P.; Goldmann, M.; Rondelez, F. *Langmuir* **1999**, *15*, 1348-1352.

(38) Langmuir, I. *Science* **1938**, *87*, 493-500.

(39) Lopez, G. P.; Biebuyck, H. A.; Frisbie, C. D.; Whitesides, G. M. *Science* **1993**, *260*, 647-649.

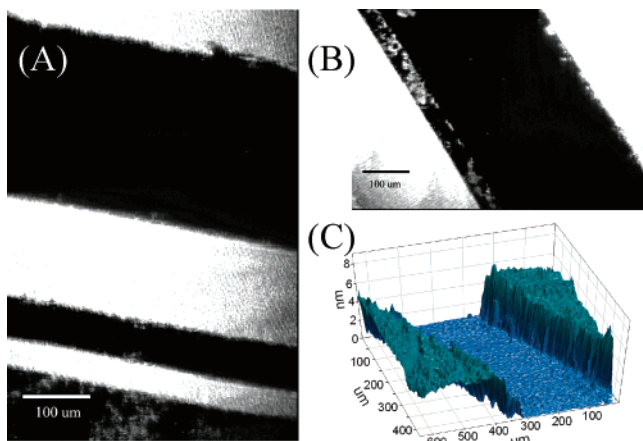


Figure 2. (A) Ellipsometric contrast image of a stripe morphology generated by two successive, rapid (60 mm min^{-1}) dipper strokes through an OTMS monolayer at 35 mN m^{-1} . Null (dark) areas represent bare silicon channels. A correlation between channel and adjacent stripe size is observed. (B) Ellipsometric contrast image and the corresponding 3D thickness plot (C) of another sample exhibiting stripe morphology. A small defect is observed at the stripe edge shown in (B) and (C).

formation, suggesting the final removal of the sample from the subphase does not affect the orientation of the striped domains.

All of the pattern structures obtained in this study showed strong thermal and chemical stability. Condensation profiles and ellipsometric imaging (see below) confirmed that the general characteristics of the patterns did not change upon multiple solvent rinses (e.g., chloroform, acetone, and ethanol), ultrasonication, and mild annealing up to 100°C for $\sim 1 \text{ h}$. Samples were observed to be stable over a period of several months under ambient conditions.

To quantitatively characterize the film morphology, imaging null-ellipsometry was used. Figure 2 shows representative 2D contrast images (Figure 2a and b) in terms of the ellipsometric angle, Δ , of a striped surface and a 3D ellipsometric thickness plot (Figure 2c). The contrast image in Figure 2b shows a single channel ($\sim 330 \mu\text{m}$) of lower ellipsometric intensity surrounded by high intensity stripes on either side. Stripe widths varied considerably from sample to sample, revealing width in a broad range of sizes from typically $50\text{--}350 \mu\text{m}$. Neighboring stripes and channels were comparable in lateral dimensions or widths. Variation in stripe width within single samples was also observed, but within a much narrower range of a few tens of micrometers. The stripes were observed over much of the macroscopic area of the substrate, excluding the edges. Moreover, the stripes were often linear over the entire width of the substrates. In multiple repetition of the experiment under otherwise identical conditions, significant variations in stripe widths and dark bands were observed to occur. Defects as well as meanderings within the stripes were also observed, reflecting presumably effects of thermal effects, defects in initial substrates, and inhomogeneities within the polymerized OTS. In all cases, however, the stripes exhibited long-range correlations.

A more detailed picture of the stripe morphology can be deduced by carefully examining the variations in ellipsometric angles in terms of film thickness changes (Figure 2c). Freshly cleaned bare silicon substrates yield the average Δ value (176.5 ± 0.5). Based on a three-phase electromagnetic model²² (air/ SiO_2 /Si), this corresponds to an oxide thickness of $\sim 20 \text{ \AA}$. In a representative LB bilayer sample, the film consists primarily of two regions: (1)

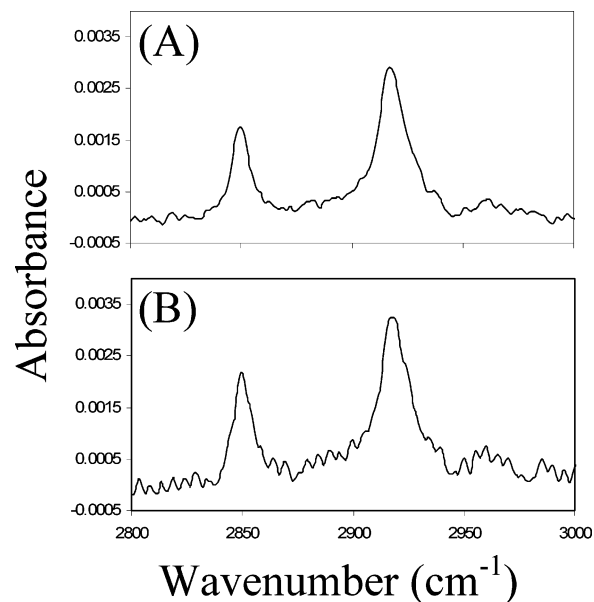


Figure 3. FT-IR spectra in the $2800\text{--}3000 \text{ cm}^{-1}$ region for (A) a uniform proximal octadecylsiloxane monolayer deposited in the first dipper upstroke and (B) the striped morphology formed after two consecutive dipper strokes. (See text for details.)

brighter stripes with an average Δ value of 171.5 ± 0.8 separated by (2) darker regions exhibiting the average Δ value of 176.4 ± 0.4 . Using a four-phase model (air/film/ 20 \AA SiO_2 /Si), the ellipsometric thickness estimates at $46.1 \pm 6.6 \text{ \AA}$ for the brighter stripe relative to the bare silicon, suggesting the formation of two noninterdigitating OTMS monolayers. The darker region corresponds to the absence of OTMS molecules within the error of our measurements.⁴⁰ Further, because the neighboring stripes and channels are of comparable width, the average film thickness is comparable to that of a single monolayer. This inference is consistent with near-zero transfer ratios observed during the downstroke (see above). Taken together, these inferences suggest that no new net material is incorporated at the substrate surface.

Figure 3 shows FT-IR spectra in the $2800\text{--}3000 \text{ cm}^{-1}$ region for the monolayer (Figure 3a) and bilayer samples (Figure 3b). Spectral envelopes are characterized by two broad peaks with peak maxima at ~ 2851 and 2919 cm^{-1} . These peaks can be assigned straightforwardly as primary contributions from the methylene C–H symmetric (d^+) and antisymmetric (d^-) stretching modes, respectively.⁴¹ A comparison of the two spectra provides important clues regarding the structures of the monolayer and striped films. First, the precise positions of these peaks are useful diagnostic markers of chain-conformation.^{42,43} The peak frequencies of the d^+ and d^- modes of alkyl chains are typically reported to be in the ranges of $2846\text{--}2850$ and $2915\text{--}2920 \text{ cm}^{-1}$ for all-*trans* extended chains and ~ 2856 and 2928 cm^{-1} for highly conformationally disordered chains, respectively. Comparison of these values with the respective values of $2850(\pm 1)$ and $2919(\pm 1) \text{ cm}^{-1}$ observed for the OTMS LB films suggest that these monolayers are

(40) Occasionally, we observed stripe samples exhibiting three regions with distinct thicknesses. In addition to the stripe and channel, there was a region bordering the stripes having an average D value of 173.71 ± 0.69 . This D value yields a thickness of $27.6 \pm 5.8 \text{ \AA}$ for the transition region (Figure 2b and c).

(41) Macphail, R. A.; Strauss, H. L.; Snyder, R. G.; Elliger, C. A. *J. Phys. Chem.* **1984**, *88*, 334–341.

(42) Snyder, R. G.; Hsu, S. L.; Krimm, S. *Spectrochim. Acta, Part A* **1978**, *34*, 395–406.

(43) Snyder, R. G.; Strauss, H. L.; Elliger, C. A. *J. Phys. Chem.* **1982**, *86*, 5145–5150.

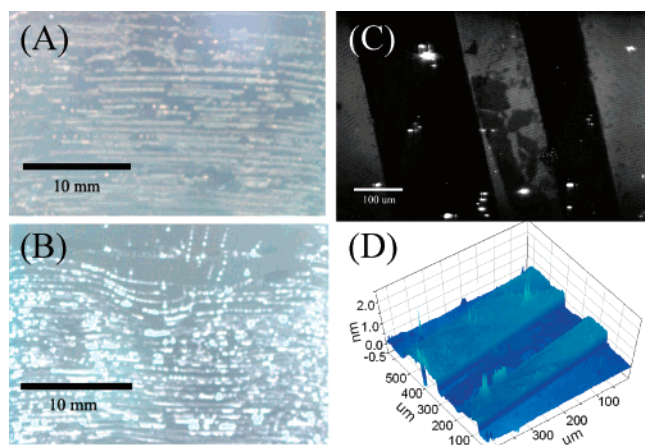


Figure 4. Optical images of striped LB substrates showing spontaneous dewetting of (A) ethanolic solution of sodium salt of fluorescein isothiocyanate (FITC) and (B) pure hexadecane. (C) Ellipsometric contrast image and (D) the corresponding 3D thickness map showing stripes and imperfections after exposure to short wavelength UV light for 90 min. Null (dark) areas represent stripe regions. The step height is observed to be ~ 5 Å for the stripe and ~ 2 – 3 Å for the imperfections. Bright white spots seen are due to dust particles present on the sample. Interference patterns from the laser illumination are visible in the off-null regions, presumably because of the low topographic and hence ellipsometric contrast between the stripe and channel regions for the ultrathin patterns of SiO_x residues. (See text for details.)

dominantly populated by all-*trans* extended chains, a structural state associated with dense packing. Second, the intensity maxima in relative absorbance for the d^+ and d^- and overall integrated intensities in the 2800–3000 cm^{-1} region are notably similar. This inference lends further support to the notion that the total number of molecules on the surface remains unchanged upon the sample downstroke as inferred from low transfer ratios observed during the second dip and ellipsometric analysis described above.

Stripe Functionalization. Samples exhibiting stripe morphologies could be further functionalized because of the strong wettability contrasts they exhibit. This was first demonstrated by exploring wettability-directed material depositions onto the striped surface by spin-coating an organic dye, fluorescein isothiocyanate (FITC), in an ethanolic solution and an oil, hexadecane. Spontaneous dewetting of the solutions occurred almost instantaneously after spin-coating, decorating the underlying pattern of substrate hydrophilicity. Figure 4a and b shows optical micrographs of FITC and hexadecane-coated striped OTMS surfaces. These images clearly show a preference of these materials in regions of compatible wettabilities: FITC was found to deposit preferentially in the hydrophilic channels, whereas hexadecane resided on the hydrophobic stripes. This preferential deposition should be applicable to a broad class of materials that display wettability preferences and can be exploited for nonlithographical patterning of materials over large areas.

In a very different type of functionalization, we performed patterned photochemistry on striped OTMS morphologies. It is well known that the exposure of thin organic films to ozone-generating UV light results in the removal of organic species, while leaving inorganic species intact. This technique has been previously applied to a wide range of monolayer systems, including alkylsilanes.^{44–46} In these cases, complete removal of the alkyl chain has been observed, leaving behind residual SiO_x films. We exposed striped OTMS patterns to ozone generating, short-

wavelength UV radiation for ~ 90 min. Figure 4c and d shows an ellipsometric contrast image and the corresponding 3D thickness plot derived by the electromagnetic analysis described earlier. These data reveal a periodic topography comprising ~ 5 Å thick stripes separated by bare SiO_2/Si regions on the substrate. This thickness is consistent with the formation of two monolayers of SiO_x as expected from the parent morphology (OTMS bilayer). Furthermore, the ellipsometric parameters for the channel regions correspond to the uncoated bare substrate, as expected. The lateral morphology of the exposed film was identical to the morphology of the striped sample prior to UV exposure. In this manner, the parent morphology is directly reflected in the pattern of SiO_x films thus formed. Occasionally, domains with thicknesses of ~ 2 – 3 Å were also observed between the striped regions (Figure 4c and d). We do not fully understand the origin of these features. However, we suspect that these features may be formed as a result of imperfections in the parent channel regions. Taken together, these data confirm that the exposure of striped samples to UV radiation results in ultrathin robust patterned SiO_x films that may be useful for biological arrays, waveguiding, and grating applications.

Discussion

Stripe Morphology. The results of the present study can be reconciled in terms of a unifying structural picture, which suggests that two consecutive dips of an SiO_2/Si substrate through a prepolymerized OTMS monolayer at an air–water interface in a rapid succession produce periodic, linear striped patterns in the LB bilayer film morphology extending over macroscopic area of the substrate surface. Below, we discuss the details of the stripe structure as determined by the collective weight of the evidence presented above.

The overall morphology comprising alternating stripes and channels was confirmed independently by condensation figures and imaging ellipsometry. The water condensation patterns in breath-tests provided the initial clues, which were further confirmed by quantitative analysis using imaging ellipsometry (Figure 2). These data show that 50–350 μm wide stripes, separated by channels of comparable widths, were obtained over the entire area of the sample surface (> 4 cm^2). The lateral dimensions or the widths of the stripes and channels varied considerably even within single samples (Figure 2a). However, neighboring stripes and channels were generally similar in width. In most cases, the stripes were linear with the exception of a few samples where meandering stripes were also observed (Figure 4b). Further, a quantitative analysis of the ellipsometric data (Figure 2c) confirmed that the brighter stripe regions (Figure 2a and b) correspond to topographically elevated regions ($\sim 46 \pm 2$ Å), consistent with two noninterdigitating OTMS monolayers. Further insight into the molecular conformational properties of the OTMS layers was provided by the positions of methylene stretching modes in FT-IR spectroscopy measurements. These data support that the striped structure comprises densely packed OTMS molecules in predominantly all-*trans* conformation. Furthermore, a comparison of the breath-tests with imaging ellipsometry⁴⁷ suggests that the elevated striped regions are relatively more

(44) Mirley, C. L.; Koberstein, J. T. *Langmuir* **1995**, *11*, 1049–1052.

(45) Ouyang, M.; Yuan, C.; Muisener, R. J.; Boulares, A.; Koberstein, J. T. *Chem. Mater.* **2000**, *12*, 1591–1596.

(46) Brunner, H.; Vallant, T.; Mayer, U.; Hoffmann, H. *Langmuir* **1996**, *12*, 4614–4617.

(47) This was accomplished by comparing the changes in the ellipsometric nulling conditions during water condensation.

hydrophobic than the channel regions. These methods for assessing wettability contrasts are qualitative and do not unequivocally distinguish between tail-to-tail or head-to-tail motifs in the bilayer. This wettability contrast was further substantiated in subsequent adsorption studies where FITC and hexadecane revealed spatially selective depositions (Figure 4a and b). Because the OTMS stripes are structurally robust and exhibit strong chemical stabilities, these stripes are useful for patterned depositions of a broad range of materials from both aqueous and organic solvents.

Implication for Formation Mechanism. Several lines of evidence help to illuminate the mechanism leading to the observed patterned morphologies. First, our data indicate a direct correlation between meniscus oscillations during the downstroke and stripe formation. Meniscus oscillations in unstable LB transfers have been generally attributed to an interplay of competing interactions involving hydrodynamic instabilities and the adhesive properties of the amphiphiles. Based on these studies, the strong adherence of amphiphiles to hydrophobic substrates during the downstroke can be expected to result in a local increase in surface energies at the moving contact line. Concomitantly, a local drop in the contact angle occurs, thereby flattening the meniscus. This tendency is counteracted by the downward motion of the substrate, which will tend to bend the meniscus. Under certain conditions, these two competing factors, such as in the present study, can lead to meniscus auto-oscillations. The observed stripe morphologies in adsorption patterns appear to mirror these oscillations. Second, meniscus oscillation in our system was observed to occur only when the proximal monolayer exhibited an ability to reorganize. This condition was met by deliberately entrapping water at the substrate–monolayer interface. This was achieved by withdrawing the substrate at large velocities (> 40 mm/min) followed by reimmersion with a short wait time (3–5 min). We believe that entrapped water inhibits covalent coupling between the film and the SiO_2/Si surface and facilitates monolayer reorganization. Third, the adsorbed amount of OTMS was found to remain unchanged before and after the downstroke. This observation points to either dynamic exchange of material at the meniscus or a concerted overturning of the extant monolayer. Local out-of-plane reorganizations of LB bilayer films have been previously reported by Takamoto et al.⁴⁸ and attributed

to the evolution of as-deposited films toward the thermodynamic equilibrium structure. In our study, the out-of-plane reorganization occurs in conjunction with a hydrodynamic instability, rather than a spontaneous restructuring of the as-formed films, and thus illustrates a different mechanism. That during the downstroke OTMS at the air–water interface is required for stripe morphology to emerge suggests the dominant role of the exchange process. We note, however, that present experiments do not fully discriminate between these two scenarios.

Taken together, these lines of evidence suggest a plausible mechanism for the formation of stripe morphology in our study. This mechanism entails combining a hydrodynamic Langmuir instability with out-of-plane reorganization of the proximal LB monolayer during the downstroke. By contrast, Gleische et al.⁷ and Badia et al.¹⁰ have exploited in-plane reorganizations, in particular, LE–LC condensation transitions, assisted by meniscus instabilities to create nanoscale stripe formation in lipid monolayers. An interesting feature of our mechanism is that it directly translates the temporal oscillatory characteristics of the meniscus to a spatial morphology of the resultant film via a concerted out-of-plane reorganization process.

Conclusion

We have described the formation of a physically robust striped morphology from a prepolymerized *n*-octadecylsiloxane monolayer at an air–water interface by rapidly withdrawing and reimmersing an oxidized silicon substrate in succession. The stripes are linear, periodic, micrometer scale in width and nanoscale in height, and exhibit an extended pattern of wettability contrasts. These stripes, comprising alternating regions of silane bilayers and the bare substrate, appear to form via a complex mechanism involving a combination of a hydrodynamic Langmuir instability and an out-of-plane reorganization. Permanent impressions of the parent striped morphology can be cast into materials exhibiting preferential adsorption characteristics and directed photochemistry.

Acknowledgment. We thank R. Sharma and D. Allara for initial discussions prompting this study. We are grateful to P. Scudder for useful discussions. Funding for this work was provided by a grant from the U.S. Department of Energy under grant # DE-FG02-04ER46173 and the NSF Center for Biophotonics Science and Technology at UC Davis. M.S.J. acknowledges support from the New College Foundation.

LA050735N

(48) Takamoto, D. Y.; Aydil, E.; Zasadzinski, J. A.; Ivanova, A. T.; Schwartz, D. K.; Yang, T. L.; Cremer, P. S. *Science* **2001**, *293*, 1292–1295.